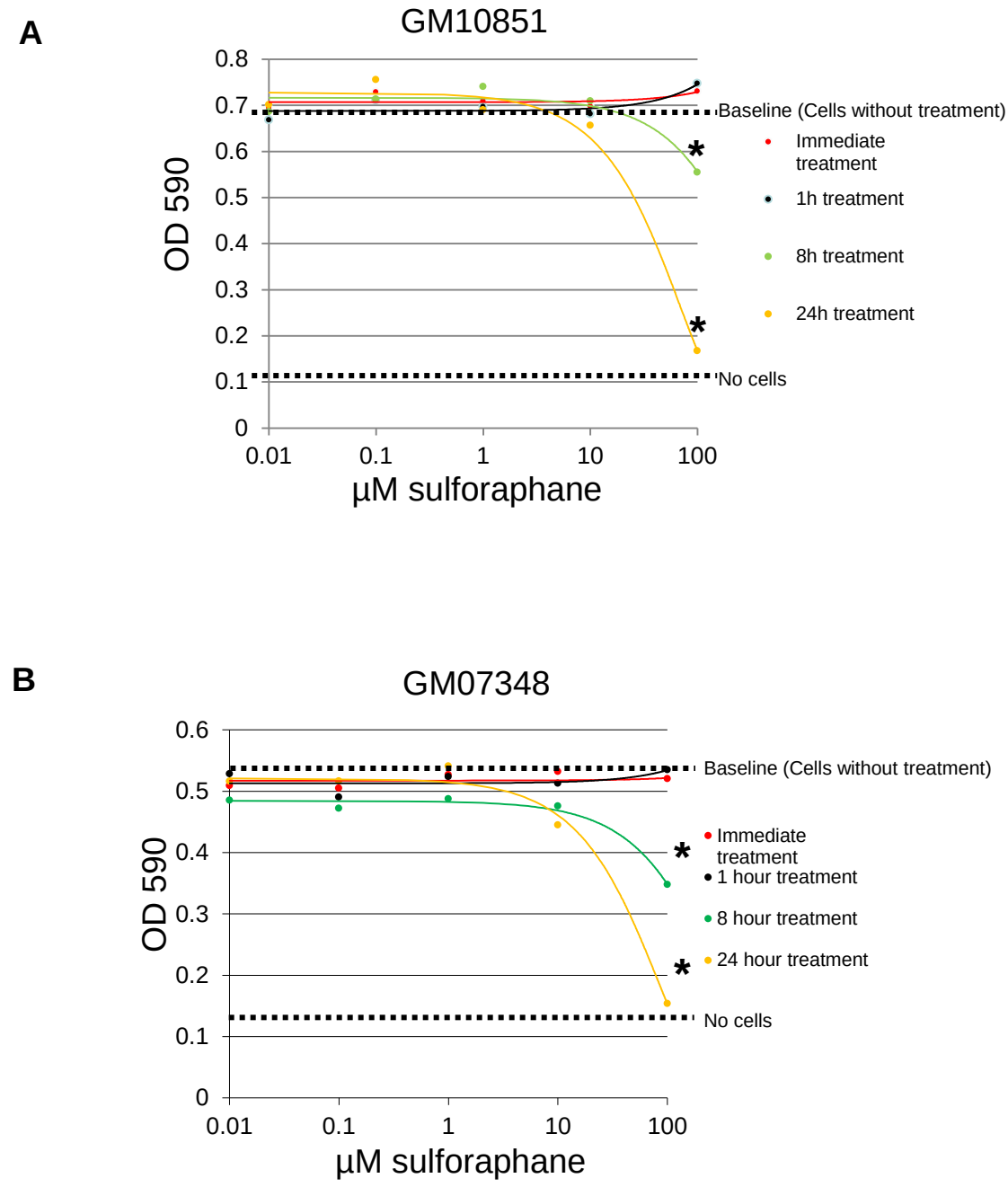

Figure S1. Cytotoxicity assay of SFN treatment in two lymphoblastoid cell lines. MTT assay (Promega) was performed following manufacturer's instructions after time (0-24 h) and dose (0.01-100 µM) SFN treatment of lymphoblastoid cells (32.5 K cell per well). For both lines, A. GM10851; B. GM07348; 8 and 24 h exposure to 100 µM SFN were cytotoxic. We chose a non-cytotoxic 5 and 24 h 10 µM exposure for our ChIP and expression experimentation, respectively.

* = $p<0.05$, versus baseline values by t-test (n=3).

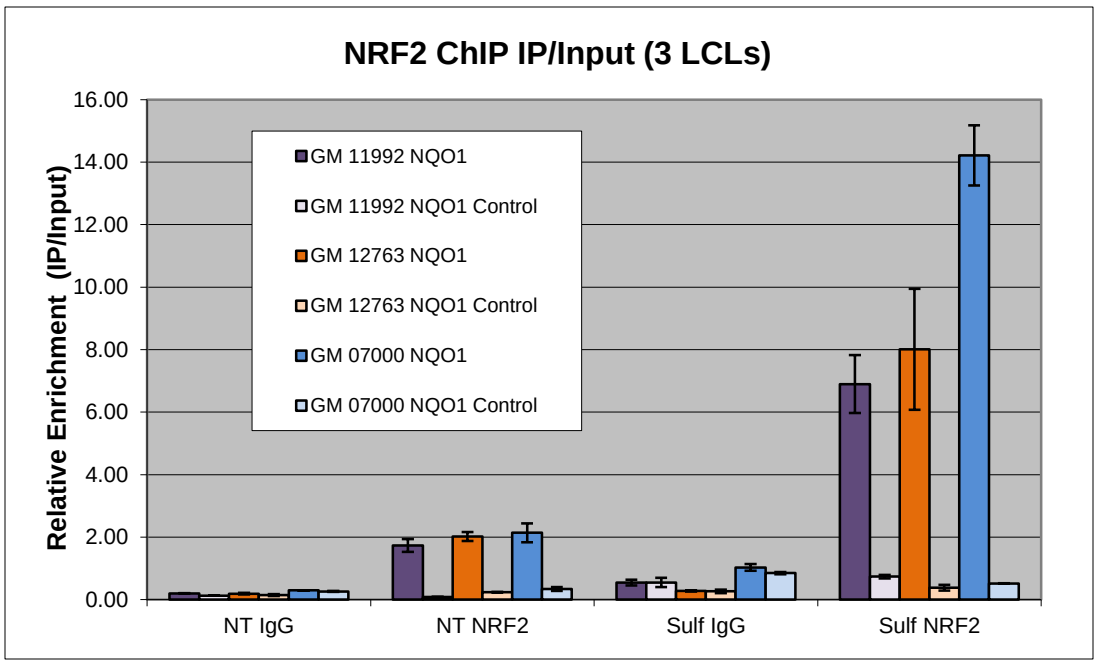

Figure S2. ChIP-PCR for NQO1 ARE region for 3 LCL demonstrates that 10 µM SFN treatment increases NRF2 binding at known ARE loci in the promoter region of *NQO1* but not at a control region 2 kb upstream (NQO1 Control). Enrichment of NQO1 over the negative control was 9.3-fold, 21.1-fold, 27.4-fold for GM11992, GM12763, and GM7000 respectively.
A small, but significant, amount of binding is also seen in vehicle control treated cells. Bars represent amplified target loci normalized to input DNA, as described in *Methods*. As controls, we IP with non-specific species-matched IgG antibody and amplify genome loci that do not have a functional ARE motif (*NQO1* promoter 2kb upstream of the functional AREs).

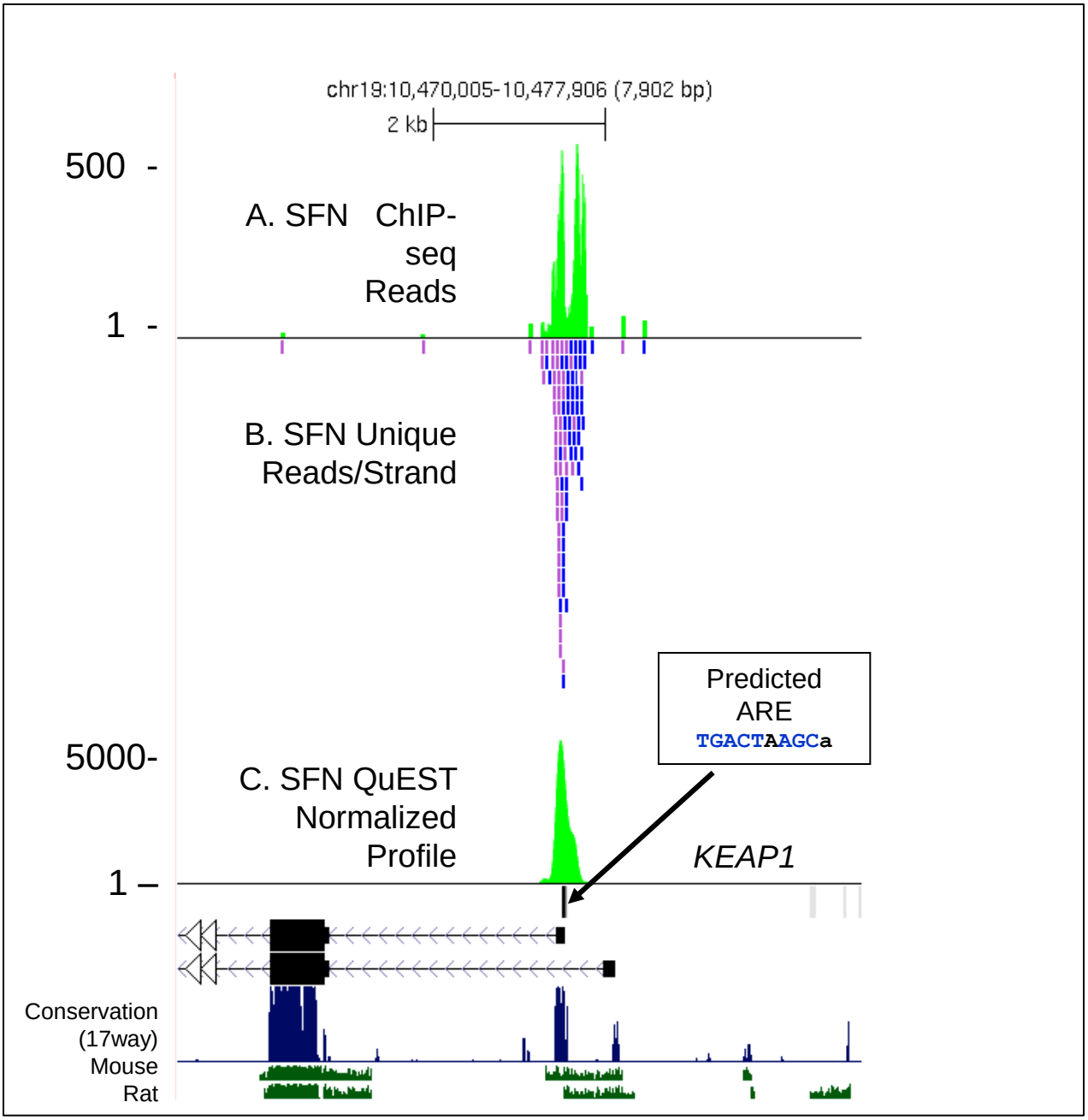

Figure S3. SFN-induced ChIP-seq reads in the *KEAP1* promoter. (*A*) All uniquely mapped sequencing reads are shown in the *KEAP1* promoter. (*B*) Displays strandedness of the sequencing reads. Plus stranded reads are *purple* and minus stranded reads are *blue.*

(C) ChIP-seq profile based on reads normalized to IgG reads and processed by QuEST. QuEST removes redundant reads and eliminates peaks that do not display reads on both strands. Location of a predicted ARE is shown under the peak. It occurs in a region of high evolutionary conservation across mammals and between rodents and humans.

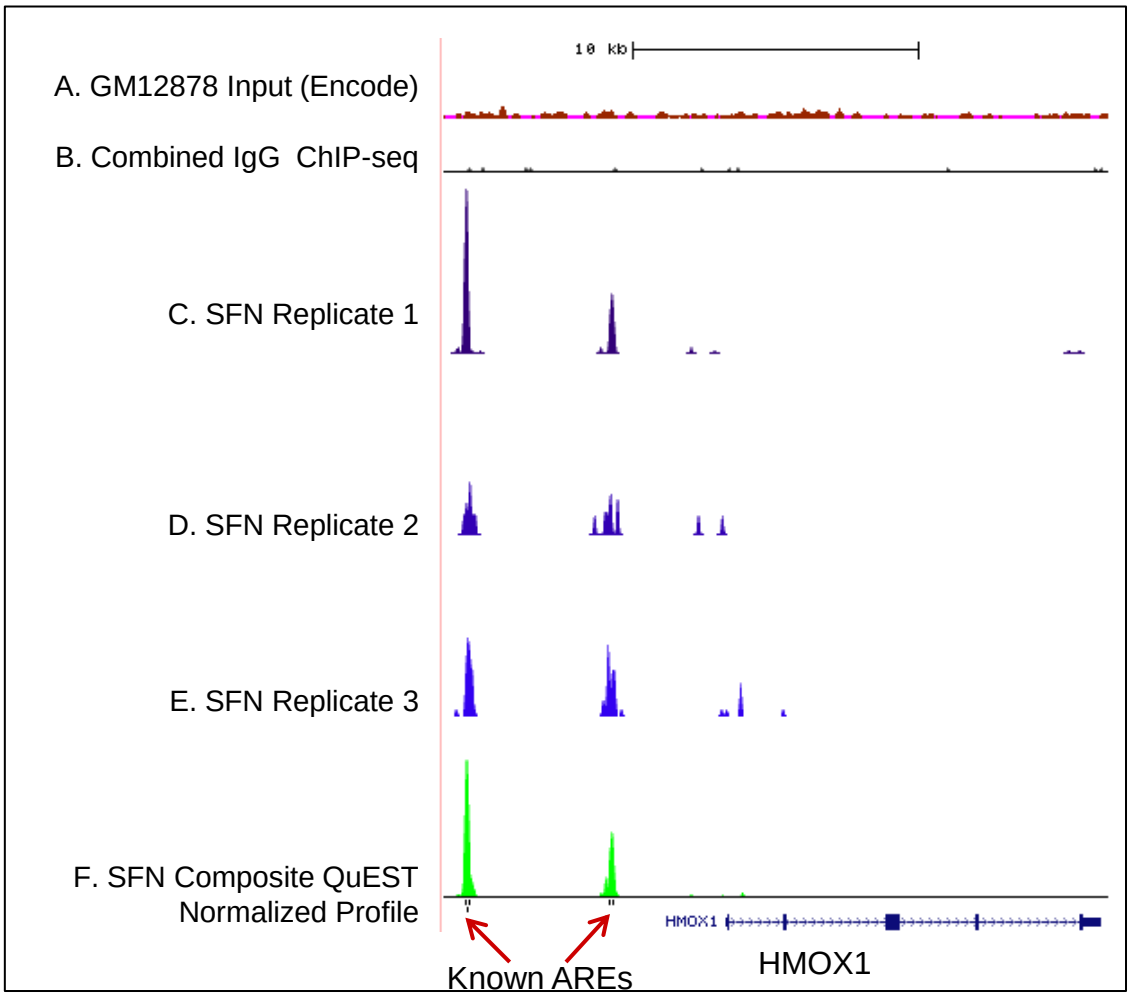

Figure S4. Replicate SFN-induced ChIP-seq peaks in the *HMOX1* promoter. To increase the depth of sequencing, reads from multiple runs were combined to created a composite profile. *A*. Encode ChIP input reads for lymphoblast cell line GM12878. (*B*) Combined IgG ChIP-seq signal for all LCLs in this study *(C-E)* SFN treated NRF2 ChIP-seq profiles for replicate sequencing runs following QuEST processing (see Figure S3). (F) SFN treated NRF2 ChIP-seq profile for pooled sequencing reads from 3 experiments following QuEST processing. Location of ARE sequences under the peaks is shown by arrows

Figure S5

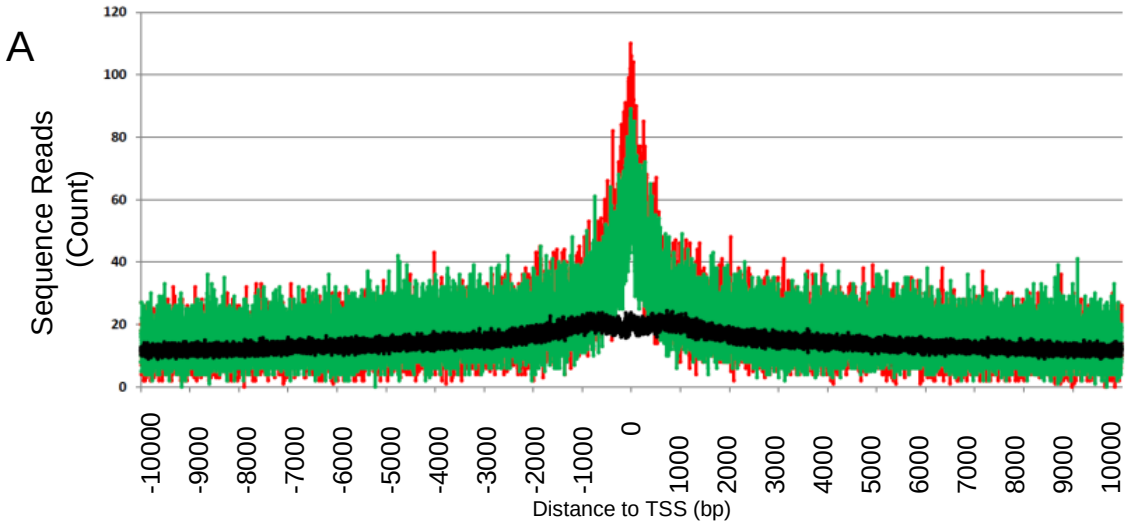

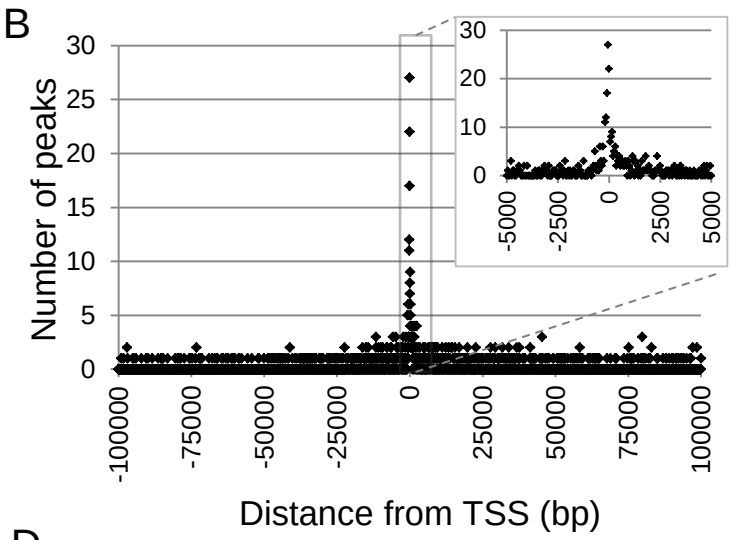

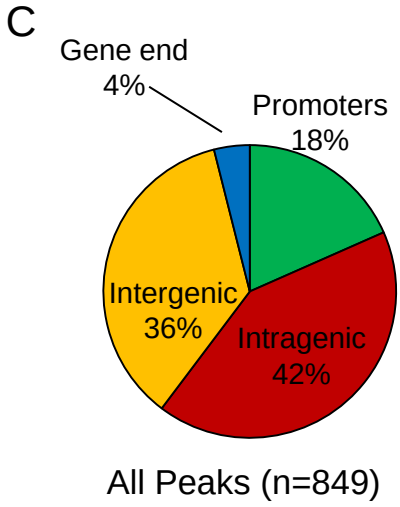

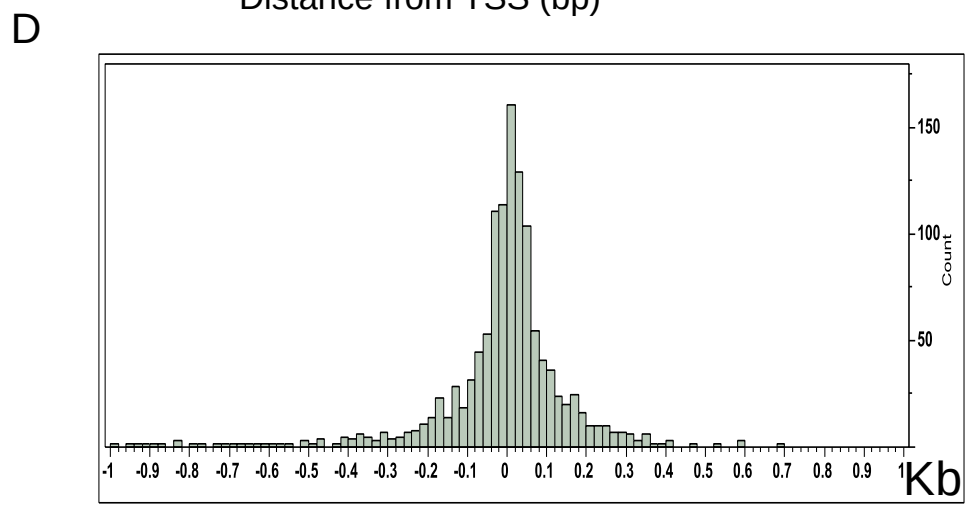

S5. ChIP-seq reveals genomic distribution of NRF2 binding sites. (A) Distribution of all sequence reads relative to nearest TSS (Black = input, green = NT, red= SFN). B. Mapped distance of ChIP-seq peak regions relative to the nearest TSS within 100 kb. Peak regions 5' of the TSS are indicated as negative numbers. Inset enlarges peak regions located within 5 kb of gene TSS. (C) Pie graph displaying genetic features for all 849 ChIP-seq peak regions including promoter (-10 kb of the TSS), intragenic, 3' end of gene (10 kb 3' to the gene end), and intergenic (outside of these defined regions) sites. . D. Distribution of 1186 identified ARE sequences relative to NRF2 ChIP-Seq peak maximum.

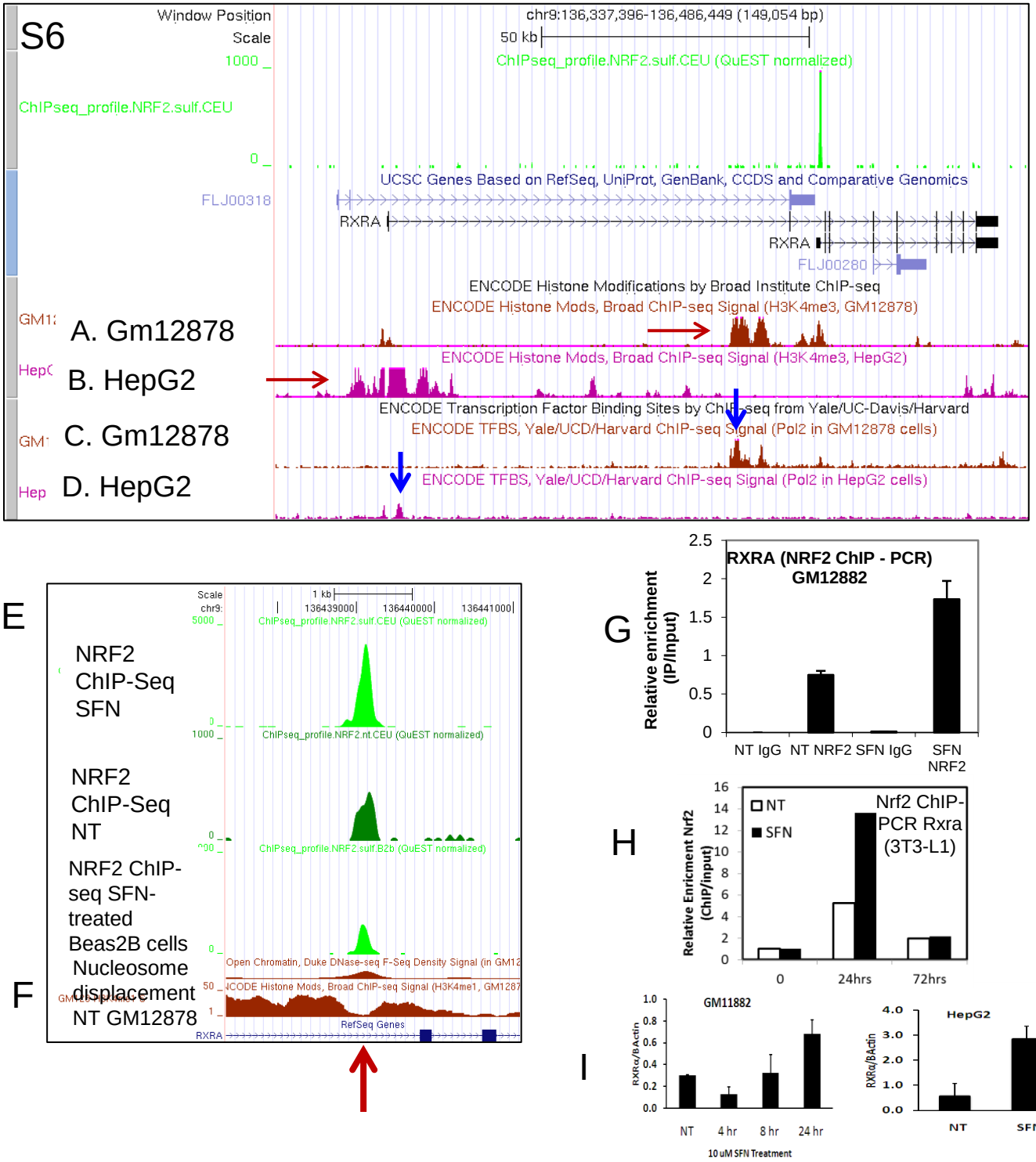

Figure S6. ENCODE histone and Pol2 ChIP-seq tracks for RXRA suggest alternate RXRA regulation in lymphoid vs HepG2 hepatocarcinoma cell lines

A. ENCODE H3K4me3 ChIP-seq in GM12878 displays open chromatin near *RXRA* Exon 2. (red arrow)
B. ENCODE H3K4me3 ChIP-seq in HepG2 cells displays open chromatin near Exon 1. (red arrow)
C. ENCODE POL2 ChIP-seq in GM12878 displays POL2 peak near RXRA Exon 2. (blue arrow)
D. ENCODE POL2 ChIP-seq in HepG2 cells displays POL2 peak near Exon 1. (blue arrow).
E. NRF2 ChIP-seq in Beas2B cells
F. ENCODE Nucleosome displacement at *RXRA* binding site (red arrow); DNase and H3K4me1 show opposing intensities indicating nucleosome displacement by NRF2 under no treatment conditions.
G. NRF2 ChIP-PCR validation of NRF2 binding RXRA following treatment with SFN in LCL.
H. ChIP-PCR validation of NRF2 binding Rxra in differentiating 3T3-L1 cells with and w/o SFN treatment .
I. RXRA mRNA expression at intervals after SFN treatment in LCLs and in HepG2 cells following SFN treatment.

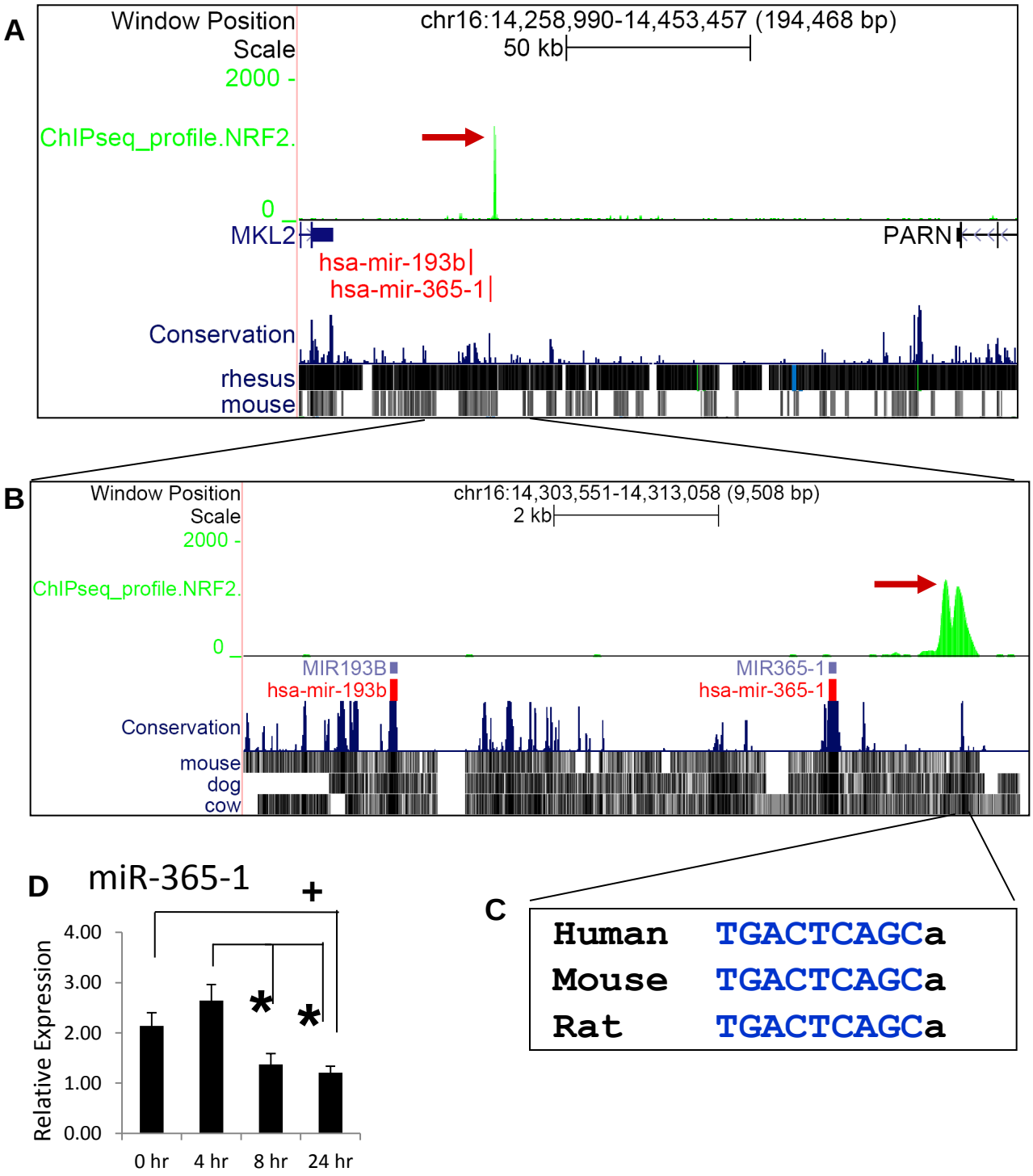

Figure S7. SFN-induced ChIP-seq peaks adjacent to the mir-193/b/mir-365-1 cluster. (*A*) mir193/b/mir-365-1 are closer to the NRF2 ChIP-seq peak (red arrow) than either of the adjacent protein coding genes (MKL2 and PARN).
.*(B)* Closeup of mir193/b/mir-365-1 region.
(C) Predicted ARE is shown under the ChIP-seq peak. It is a perfect match with the consensus and occurs in a narrow region of high evolutionary conservation across mammals and between rodents and humans.
(D) Expression of miR-365-1 was measured in triplicate, relative to zero time point, changes observed were not significant by t-test (+, p=0.053). Both 8, 24 hr were significantly lower than 4 hr (*, p = 0.035).

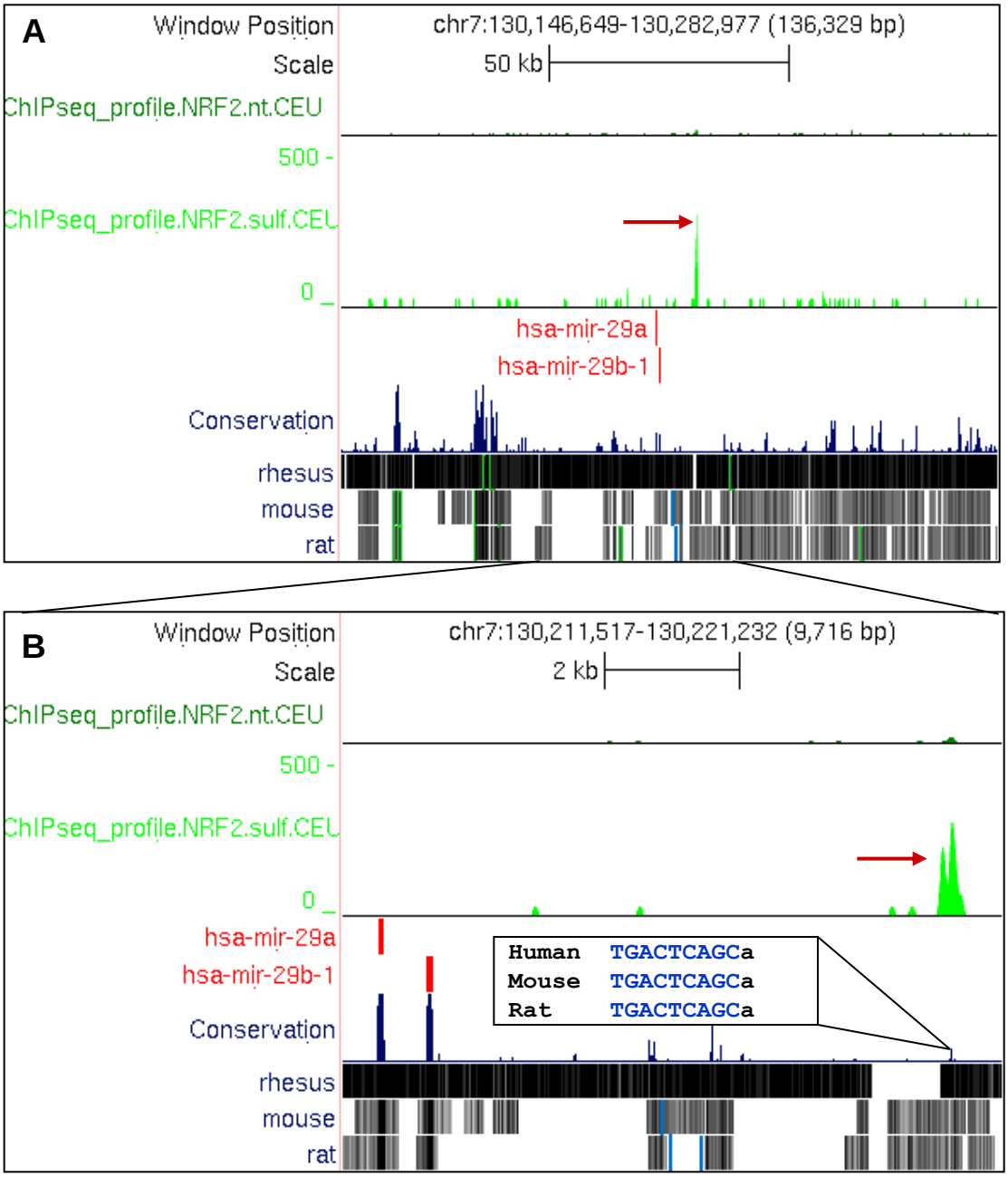

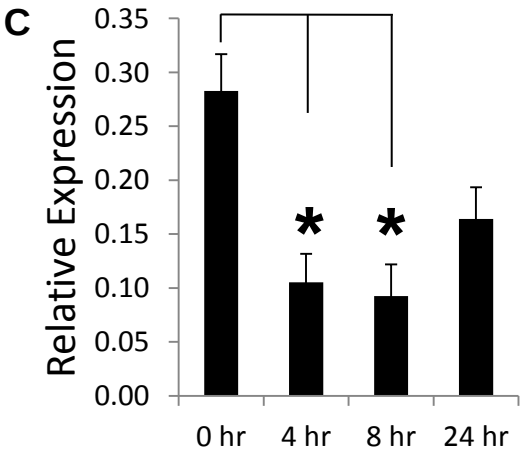

Figure S8. SFN-induced ChIP-seq peaks adjacent to the mir-29A/29B cluster.

A. Mir-29A/29B are proximal to the NRF2 ChIP-seq peak (red arrow). B. Closeup of mir29 region, (Insert) Predicted ARE is shown under the ChIP-seq peak. It is a perfect match with the consensus and occurs in a narrow region of high evolutionary conservation across mammals and between rodents and humans.

C. MiR-29B displays significantly reduced expression following SFN treatment. Triplicate cultures, * $p<0.05$

Figure S9.

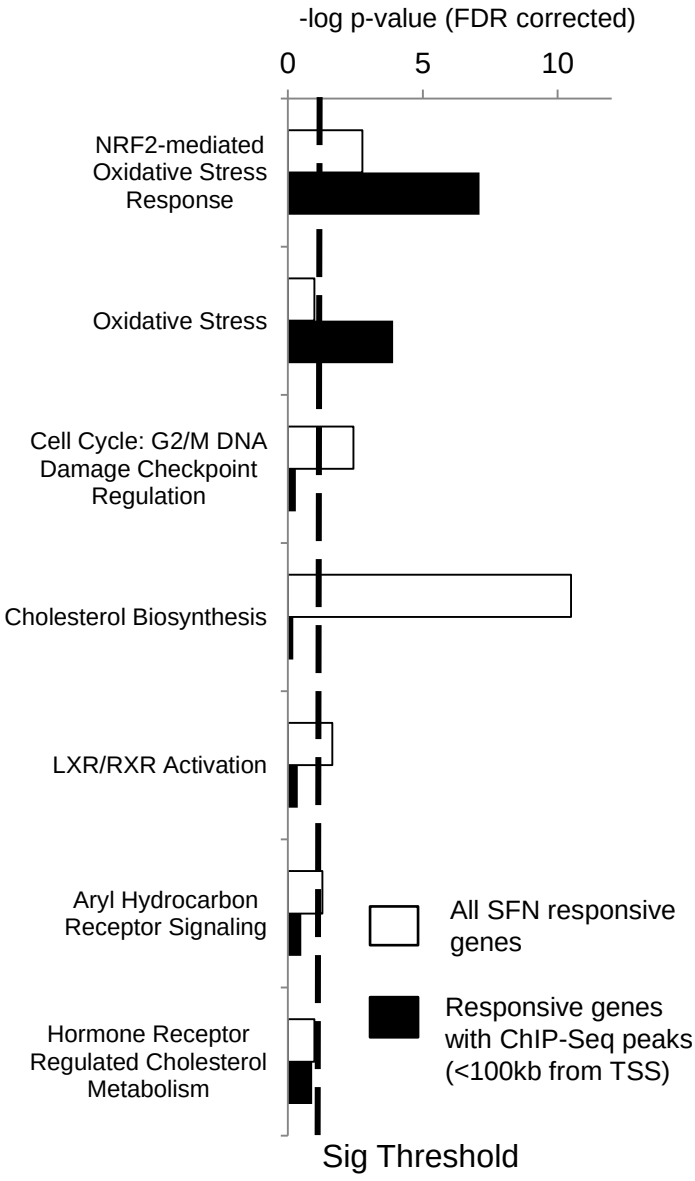

Figure S9. Pathway analysis of SFN-responsive gene expression and SFN-responsive genes with ChIP-seq peak regions reveals NRF2 pathway enrichment. Ingenuity pathway analysis of 508 SFN-responsive genes displays enrichment for 5 pathways in the toxicity response pathway list (open bars), whereas the 77 SFN-responsive genes that have ChIP-seq peak regions within 100 kb of the TSS were enriched for only the 2 pathways related to oxidative stress (dark bars). Plotted are FDR corrected p-values. Dotted line represents threshold of significance ($p<0.05$). Cholesterol biosynthesis pathway has only 16 members; of these, 10/16 showed altered expression but only 1 had a ChIP-seq peak. Similarly, cell cycle genes were enriched among SFN responsive genes but not ChIP-seq.

Figure S10.

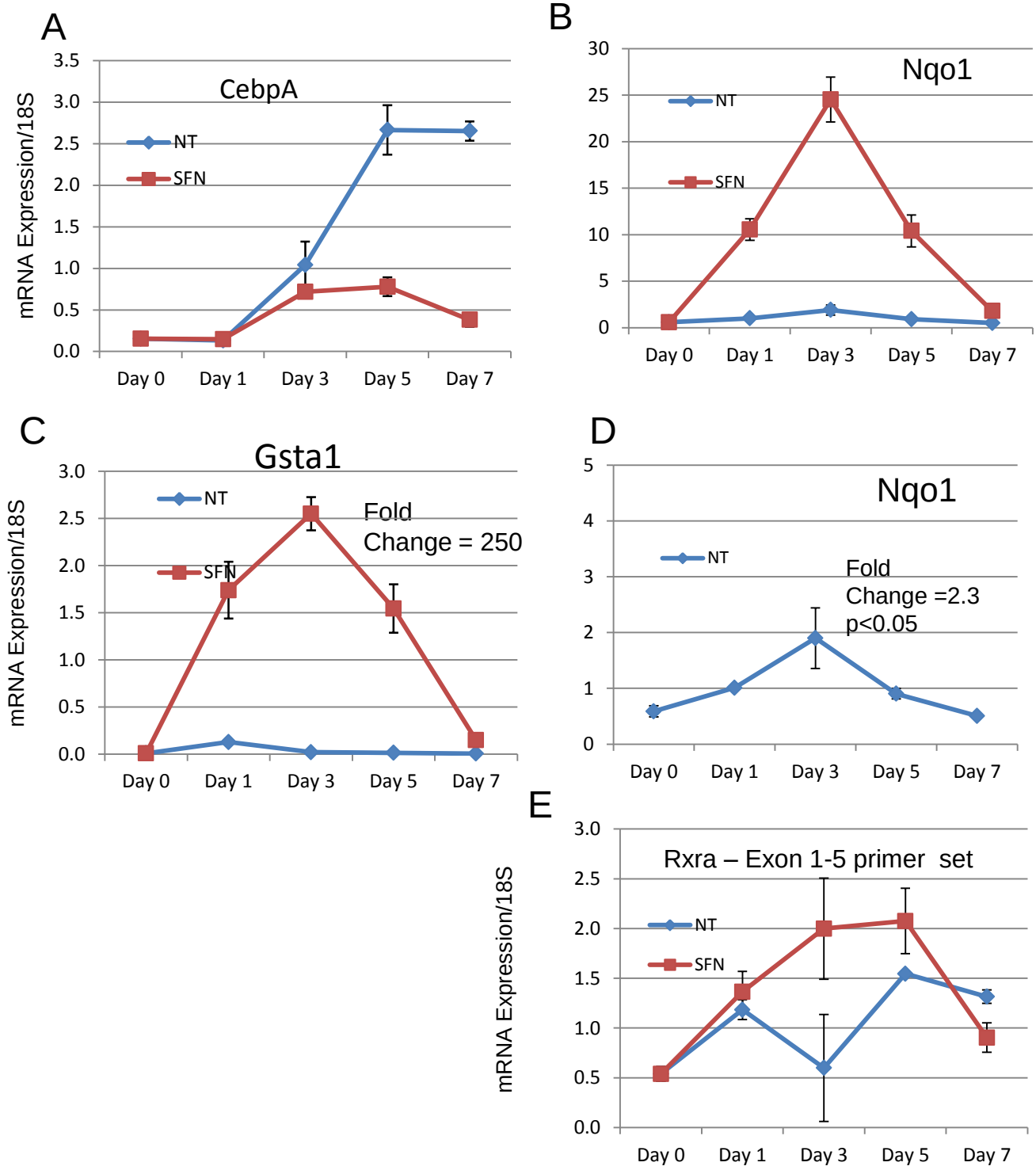

Figure S10. Effects of SFN treatment (red squares) on 3T3-L1 adipocytes during differentiation. Blue curves (NT) are standard differentiation conditions with DMI. A. CebpA expression by realtime PCR increases rapidly following day 3 under standard differentiation conditions indicating commitment to terminal state. Continuous SFN treatment prevents differentiation. Both Nqo1 (B) and Gsta1 (C) show large, rapid increases following SFN treatment. D. Nqo1 increases significantly during DMI induced differentiation E) Rxra expression is higher under SFN treatment conditions using a primer set that detects mRNA containing exons 1 to 5. (similar to Figure 6D)

Supplementary Table S1. Sequencing reads from NRF2 ChIP in HapMap cell lines, total and uniquely mapped.

Sample (Cell line ID)	Total reads	Uniquely mapped		
GM11994	4766716	218907	(Pilot Study)	Vehicle only NRF2 IP
GM11992	14487710	9908849		Vehicle only NRF2 IP
GM12763				Vehicle only NRF2 IP
GM06993	11803840	8848929		Vehicle only NRF2 IP
GM12872				Vehicle only NRF2 IP
GM07000	8704444	6695890		Vehicle only NRF2 IP
GM11882				Vehicle only NRF2 IP
GM11994	6416702	2224386	(Pilot Study)	SFN NRF2 IP
GM11992	9340414	5409838		SFN NRF2 IP
GM12763				SFN NRF2 IP
GM06993	9635203	7377230		SFN NRF2 IP
GM12872				SFN NRF2 IP
GM07000	14919604	11511264		SFN NRF2 IP
GM11882				SFN NRF2 IP
All (Veh)	16389204	13005281		IgG IP
All (SFN)	15233016	11956985		IgG IP
All (Veh)	36143825	28153841		Input
All (SFN)	44530147	33968628		Input

Supplementary Table S2. Effect of negative control sequence reads on peak detection using QuEST.

In order to test the effect of different sources of control sequencing reads on peak detection by QuEST, we compared peak detection when using reads from sequencing of input DNA with reads from sequencing a pool of ChIP DNA from several IgG ChIP reactions. The table displays the number of NRF2 bound regions (peaks) detected using the following as a reference control sample: IgG reads (present study); input reads (present study), GM12878 input; pool of input of lymphoblast lines (listed below).

The control read source made very little difference in the total number of peaks detected. The alignment of 36-base sequence reads of Input DNA were downloaded from the Encode project website (http://hgdownload.cse.ucsc.edu/goldenPath/hg18/encodeDCC/wgEncodeUwChIPSeq/). The following 4 files were used, including:
wgEncodeUwChIPSeqAlignmentsGm12872Input.tagAlign,
wgEncodeUwChIPSeqAlignmentsGm12873Input.tagAlign,
wgEncodeUwChIPSeqAlignmentsGm12874Input.tagAlign,
wgEncodeUwChIPSeqAlignmentsGm12875Input.tagAlign.

	Reference Sequence Reads			
	IgG (this study)	**Input (this study)**	**input GM12878 (ENCODE)**	**inputs (pool of 4 lines, ENCODE)**
NRF2sulf ChIP-Seq Peaks	836	849	836	841
Peaks in Common with NRF2sulf vs IgG		788	794	797

NRF2 ChIP-on-chip compared with ChIP-seq. In parallel to our ChIP-seq study we performed NRF2 ChIP-on-chip with the Agilent Human Promoter Array. This array has limited genomic coverage, containing tiled probes for locations between -5.5 kb upstream and +2.5 kb downstream of the TSS of approximately 17,000 genes. We treated one LCL in biological triplicate with either 0.1% DMSO or 10 µM SFN. Similar to ChIP-seq, we also immunoprecipitated ChIP DNA with non-specific IgG antibody as a negative control and hybridized this DNA to the array. After eliminating regions in common with IgG, we observed 534 ChIP-on-chip regions near 272 genes (Supplementary Data File 4). There were 285 genes with ChIP-seq regions within -5.5-kb and +2.5-kb of the TSS (the range of the ChIP-on-chip). However, when we compare the two datasets, we observed that only 47 of the 272 (17.2%) genes with ChIP-on-chip regions also have ChIP-seq regions in SFN-treated LCLs. Considering ARE motifs, the HC ChIP-seq regions were far more likely to contain AREs than the ChIP-on-chip regions (99%, 234/237 vs 56%, 297/534). We used the ChIP-on-ChIP data as a secondary means of validating candidate genes. Genes that overlap between ChIP-seq and ChIP-on-chip are listed in Supplemental data file 1.

Supplementary Table S3. List of known human ARE genes. ARE validated by deletion/mutation constructs (DM), electrophoretic mobility shift assay (EMSA), reporter gene assay (RGA), and/or chromatin immunoprecipitation assay (ChIP).

Gene	Sequence	Validation	References	NRF2 ChIP-seq region ID(s)
ARE consensus	**RTKAYnnnGCR**	-	(Erickson et al 2002)	**-**
ABCB11	CCAAGGTGAATCAGCAATTTC	DM,EMSA,CHIP	(Weerachayaphorn et al 2009)	-
ABCC1	TCTGTGTGACTCAGCTTTGGA	NPA,EMSA,RGA	(Kurz et al. 2001)	-
AKR1C1	TCAGGGTGACTCAGCAGCTTG	DM,EMSA,RGA,CHIP	(Lou et al. 2006)	-
AKR1C2	TCAGGGTGACTCAGCAGCTTG	DM,EMSA,RGA, CHIP	(Lou et al. 2006)	-
APOA1	CAGCTCTGTCCCTGGGGCTGG	DM, EMSA, RGA	(Mooradian et al. 2006)	-
ATF3	TTAAGGTGACACAGCATCTAA	DM,RGA,CHIP	(Kim et al. 2010)	-
CES1A1	AGATCGTGAGACAGCATTAAT	DM,EMSA,RGA,CHIP	(Maruichi et al. 2010)	-
ETS1	AGCGGGTGACCAAGCCCTCAA	DM,EMSA,RGA	(Wilson et al. 2005)	-
FTH1-1	CCTCCATGACAAAGCACTTTT	DM,EMSA,RGA,CHIP	(Tsuji 2005)	P-4-1
FTH1-2	CCACCGTGACTCAGCACTCCG	DM,EMSA,RGA,CHIP	(Tsuji 2005)	P-4-1
FTL	TCAGCATGACTCAGCAGTCGC	DM,RGA	(Hintze and Theil 2005)	P-2-1
GCLC	TCCCCGTGACTCAGCGCTTTG	DM,EMSA,RGA	(Mulcahy et al. 1997; Wild et al. 1998)	P-18-2
GCLM-1	TAACGGTTACGAAGCACTTTC	DM,EMSA,RGA	(Moinova and Mulcahy 1998; Erickson et al. 2002)	P-75-2
GCLM-2	AGACAATGACTAAGCAGAAAT	DM,EMSA,RGA	(Moinova and Mulcahy 1998; Erickson et al. 2002)	P-75-2
GNAI2	AGCCTGTGACTGGGCCGGGGC	DM,EMSA,RGA,CHIP	(Arinze and Kawai 2005)	-
GPX2	CCAGGATGACTTAGCAAAAAC	DM,EMSA,RGA,CHIP	(Banning et al. 2005)	-
GSTP1	GCGCCGTGACTCAGCACTGGG	DM,EMSA,RGA	(Montano et al. 2004)	P-90-1
HMOX1-1	GGACCGTGACTCAGCAGGAAA	RGA, CHIP	(Keum et al. 2006)	P-10-2
HMOX1-2	GGACCGTGACTCAGCGAAAAC	RGA, CHIP	(Keum et al. 2006)	P-10-2
HMOX1-3	AGACCGTGACTCAGCGAAAAC	RGA, CHIP	(Keum et al. 2006)	P-10-2
KRT16	GAACCTGGAGTCAGCAGTTAG	DM,EMSA,RGA	(Endo et al. 2008)	-
MAFG	TCACGCTGACTCAGCACATTG			P-84-2, P-103-2
ME1	CTGCCATGACTCAGCGCTTCT			P-27-2
NQO1	TCACAGTGACTCAGCAGAATC	DM,EMSA,RGA, CHIP	(Li and Jaiswal 1992; Dhakshinamoorthy et al. 2005)	p-5-3
NQO2	AGGTGGTGATGTTGCATCACA	DM,EMSA,RGA,CHIP	(Wang and Jaiswal 2006)	-
PRDX1	TGTAACTGAATCAGCATCAGC	DM,EMSA,RGA,CHIP	(Kim et al. 2007)	P-31-2*
PRDX6	GCAACGTGACCGAGCCCCGCA	DM,RGA,CHIP	(Chowdhury et al. 2009)	-
PSMA3	AGCCAATGAGCGGGCCTGTTA	DM, EMSA, RGA	(Takabe et al. 2006)	P-193-2
PTGS2	TTTTAGTGACGACGCTTAATA	RGA	(Sherratt et al. 2003)	-
S100A6	GACACGTGACTCGGCAAGGGG	DM,EMSA,RGA	(Lesniak et al. 2005)	-
SAT	CCGCTATGACTAAGCGCTAGT	DM,NPA,EMSA,RGA	(Wang et al. 1998)	-
SRXN1	CCAGGGTGAGTCGGCAAAGCC	DM, RGA, CHIP	(Singh et al. 2009)	p-33-1
SOD1	AACTAATGACATTTCTAGACA	DM, EMSA, RGA	(Park and Rho 2002; Dreger et al. 2009)	-
TBXAS1	AAGGAATGAATCAGCAACTTT	DM,EMSA,RGA,CHIP	(Yaekashiwa and Wang 2002)	P-802-1,P-3089-1*
TXN	TCACCGTTACTCAGCACTTTG	DM,EMSA,RGA	(Kim et al. 2003)	p-9-3
TXNRD1-1	TCATTCTGACTCTGGCAGTTA	DM,EMSA,RGA	(Hintze et al. 2003)	P-20-1, P-186-1
TXNRD1-2	TCAGAATGACAAAGCAGAAAT	DM,EMSA,RGA	(Hintze et al. 2003)	P-20-1, P-186-1
UGT1A1	AAACCCGGACTTGGCGCTTGG	DM,RGA,EMSA	(Yueh and Tukey 2007)	-
UGT1A6	GAAAGCTGACACGGCCATAGT	DM,EMSA,RGA	(Munzel et al. 2003)	-
UGT1A6	TCTGTCTGACTTGGCAAAAAT	DM,EMSA,RGA	(Munzel et al. 2003)	-
UGT2B7	AACTACTGACTCGGCTGGTCT	DM, EMSA	(Nakamura et al. 2008)	-

***** ChIP-seq peak region does not match ARE locus cited in literature

Supplementary Table S4. SFN-responsive genes with ChIP-seq peak regions in lymphoblastoid cells.

Gene	Gene ID	Chromosome	Average expression intensity (log2)		Fold change	ChIP-seq Peak ID(s)	
			Vehicle only	SFN			
HMOX1	3162	chr22	7.4	11.0	12.2	P-10-2	upregulated
NQO1	1728	chr16	8.8	11.2	5.3	P-5-3	
AMBP	259	chr9	5.4	7.4	4.0	P-1900-1	
SQSTM1	8878	chr5	8.2	9.6	2.7	P-24-1	
ABCB6	10058	chr2	7.4	8.8	2.6	P-56-2	
FTH1	2495	chr11	9.0	10.4	2.6	P-4-1 P-5748-1	
COL24A1	255631	chr1	6.9	8.2	2.5	P-157-1	
SRXN1	140809	chr20	7.5	8.8	2.4	P-33-1	
OSGIN1	29948	chr16	5.6	6.8	2.4	P-523-1	
TXNRD1	7296	chr12	8.7	9.8	2.1	P-20-1 P-186-1	
CTSC	1075	chr11	9.9	11.0	2.1	P-1117-1 P-2918-1	
AGPAT9	84803	chr4	6.2	7.2	2.0	P-145-1	
MSC	9242	chr8	9.6	10.6	2.0	P-122-1	
SH3TC1	54436	chr4	8.2	9.2	2.0	P-6104-1	
GCLM	2730	chr1	8.6	9.5	2.0	P-75-2	
HSPA1B	3304	chr6	9.1	10.0	1.9	P-3028-1 P-1408-1	
GABARAPL1	23710	chr12	7.1	8.0	1.9	P-2825-1	
ABHD4	63874	chr14	6.1	7.0	1.8	P-2768-1	
CLIP4	79745	chr2	6.7	7.5	1.8	P-109-2	
PIR	8544	chrX	9.5	10.3	1.8	P-30-1 P-4173-1	
ME1	4199	chr6	8.1	8.9	1.8	P-27-2	
DUSP5	1847	chr10	10.3	11.2	1.8	P-710-1 P-127-2 P-1087-1	
IDS	3423	chrX	8.9	9.7	1.6	P-32476-1	
SLC12A8	84561	chr3	8.7	9.4	1.6	P-3139-1	
GCLC	2729	chr6	6.7	7.4	1.6	P-18-2	
CD27	939	chr12	10.2	10.8	1.6	P-150-1	
MAFG	4097	chr17	6.8	7.5	1.6	P-103-2 P-84-2	
UNKL	64718	chr16	7.0	7.7	1.5	P-38-2	
LTA	4049	chr6	7.8	8.4	1.5	P-40771-1	
GPNMB	10457	chr7	6.4	7.0	1.5	P-764-1	
RXRA	6256	chr9	8.3	8.9	1.5	P-3113-1 P-8-2	
PMAIP1	5366	chr18	7.6	8.2	1.5	P-1767-1 P-405-1 P-42-1 P-24021-1	
PRDM1	639	chr6	8.2	8.8	1.5	P-6737-2	
SARM1	23098	chr17	6.4	7.0	1.5	P-2965-1	
SLC3A2	6520	chr11	7.6	8.1	1.4	P-489-3	
TALDO1	6888	chr11	12.1	12.6	1.4	P-2563-1 P-2735-1	
P2RY10	27334	chrX	8.9	9.4	1.4	P-393-2	
HTATIP2	10553	chr11	7.9	8.4	1.4	P-69-2	
FAM167A	83648	chr8	6.6	7.1	1.4	P-5479-2 P-3048-1	

Supplementary Table S4. SFN-responsive genes with ChIP-seq peak regions in lymphoblastoid cells. (cont.)

Gene	Gene ID	Chromosome	Average expression intensity (log2) Vehicle only	Average expression intensity (log2) SFN	Fold change	ChIP-seq Peak ID(s)	
IGF2R	3482	chr6	9.8	10.3	1.4	P-141-1	upregulated
BTG2	7832	chr1	9.8	10.2	1.4	P-129-2	
KEAP1	9817	chr19	7.5	8.0	1.4	P-11-2	
AIFM2	84883	chr10	6.3	6.8	1.4	P-77-1	
TFE3	7030	chrX	6.4	6.9	1.4	P-295-2	
TXN	7295	chr9	13.1	13.6	1.4	P-9-3	
TNFSF9	8744	chr19	9.4	9.9	1.4	P-32468-1	
TBXAS1	6916	chr7	7.3	7.8	1.4	P-3089-1	
EXOC7	23265	chr17	9.2	9.6	1.4	P-108-2	
GSR	2936	chr8	8.9	9.3	1.4	P-25-1 P-521-1	
SLC16A6	9120	chr17	6.7	7.1	1.4	P-1956-1	
GDF15	9518	chr19	6.5	6.9	1.4	P-195-1	
TINAG	27283	chr6	6.2	6.6	1.4	P-4921-2	
ATF3	467	chr1	8.7	9.1	1.4	P-6169-1	
EDA2R	60401	chrX	5.9	6.3	1.3	P-1799-1	
PIP5K1C	23396	chr19	7.8	8.2	1.3	P-48-1	
GCNT3	9245	chr15	6.5	6.9	1.3	P-265-2	
BEND6	221336	chr6	6.1	6.5	1.3	P-180-1	
RFFL	117584	chr17	8.7	9.1	1.3	P-254-3 P-4828-1	
TRIM69	140691	chr15	7.7	8.1	1.3	P-2986-1	
COCH	1690	chr14	9.5	9.9	1.3	P-2600-1	
HRASLS2	54979	chr11	6.3	6.7	1.3	P-156-1	
FBXO30	84085	chr6	7.7	8.1	1.3	P-2747-1	
KIAA1370	56204	chr15	8.1	8.5	1.3	P-2468-1	
CTTN	2017	chr11	7.7	8.1	1.3	P-3907-1	
IRF4	3662	chr6	10.1	10.4	1.3	P-33374-1	
RNF121	55298	chr11	7.5	7.9	1.3	P-1142-1	
FECH	2235	chr18	7.6	8.0	1.3	P-260-1	
SLC3A2	6520	chr11	9.3	9.7	1.3	P-489-3	
WDR81	124997	chr17	6.2	6.6	1.3	P-128-1	
COLEC12	81035	chr18	5.6	6.0	1.3	P-20991-1	
HIST1H1C	3006	chr6	11.9	10.8	0.5	P-2886-2	downregulated
DLGAP5	9787	chr14	10.3	9.3	0.5	P-1835-1	
C5orf13	9315	chr5	9.6	8.6	0.5	P-5194-1	
MT2A	4502	chr16	10.0	9.2	0.5	P-30518-1	
INSIG1	3638	chr7	11.2	10.4	0.6	P-375-1	
RAB33A	9363	chrX	8.7	7.9	0.6	P-5466-1	
AURKB	9212	chr17	10.8	10.1	0.6	P-5975-1	
PRC1	9055	chr15	10.8	10.2	0.7	P-7681-1	
PSAT1	29968	chr9	9.9	9.3	0.7	P-4660-1	
HMHB1	57824	chr5	7.2	6.7	0.7	P-530-1	
RAB31	11031	chr18	9.5	9.0	0.7	P-778-1	
DUSP22	56940	chr6	8.9	8.4	0.7	P-1738-2 P-7122-1	
NCAPD2	9918	chr12	10.2	9.7	0.7	P-1820-1	

Supplementary Table S5. Expression of known/putative ARE genes in NRF2-silenced cell lines.

		Expression values (normalized to β-actin x100)								
		Control siRNA			NRF2 siRNA					
Gene Name	Cell line	Baseline	SFN	% change up/down	Baseline	% of control siRNA		SFN	% of control siRNA	
NFE2L2 (NRF2)	A549	83.7	115.2	**137.6%***	3.9	**4.6%**	*	6.7	**5.8%***	
	BEAS-2B	37.4	50.1	134.2%	9.7	**25.9%**	*	6.8	**13.5%***	
FTH1	A549	4.5	2.9	**63.8%***	4.4	98.2%		4.1	142.7%	Known ARE genes
	BEAS-2B	2.2	4.2	**188.2%***	3.3	149.0%		2.8	**66.2%***	
FTL	A549	110.6	89.5	81.0%	12.7	**11.5%**	*	13.2	**14.8%***	
	BEAS-2B	426.3	1031.6	**242.0%***	138.4	**32.5%**	*	187.5	**18.2%***	
HMOX1	A549	7.7	10.6	**138.4%***	0.8	**10.3%**	*	0.5	**4.8%***	
	BEAS-2B	3.7	76.6	**2062.4%***	3.3	89.4%		13.4	**17.5%***	
NQO1	A549	6555.3	5925.3	**90.4%***	1205.1	**18.4%**	*	1132.9	**19.1%***	
	BEAS-2B	231.7	722.8	**312.0%***	97.7	**42.2%**	*	92.6	**12.8%***	
PRDX1	A549	1.6	1.1	**69.3%***	0.2	**11.1%**	*	0.2	**15.1%***	
	BEAS-2B	0.4	0.8	**172.3%***	0.3	**76.5%**	*	0.4	**58.5%***	
PSMA3	A549	33.7	26.6	**79.0%***	22.0	**65.2%**	*	17.0	64.1%*	
	BEAS-2B	30.0	28.0	93.5%	17.6	**58.6%**	*	13.3	**47.5%***	
KEAP1	A549	11.1	11.7	105.6%	3.7	**33.7%**	*	2.8	**24.1%***	Putative ARE genes
	BEAS-2B	11.7	13.7	116.7%	8.1	**68.6%**	*	8.6	**62.9%***	
MAFG	A549	2.2	3.0	**136.1%***	0.0	**2.0%**	*	0.1	**1.8%***	
	BEAS-2B	0.3	1.7	**567.2%***	0.1	**38.1%**	*	0.3	**16.7%***	
OSGIN1	A549	24.3	42.7	**175.7%***	0.6	**2.6%**	*	0.5	**1.1%***	
	BEAS-2B	0.4	4.8	**1295.9%***	0.1	**29.7%**	*	0.7	**14.2%***	
PIR	A549	15.0	16.0	106.7%	12.6	84.3%		16.5	102.8%	
	BEAS-2B	0.0036	0.02	**548.3%***	0.00074	**20.7%**	*	0.0025	**12.5%***	
SLC7A11	A549	1.1	1.4	**134.9%***	0.2	**17.8%**	*	0.1	**6.1%***	
	BEAS-2B	0.3	4.6	**1490.0%***	0.3	108.1%		1.1	**22.9%***	
TALDO1	A549	17.3	14.1	81.7%	4.3	**24.7%**	*	3.1	**21.6%***	
	BEAS-2B	9.3	10.9	117.6%	5.0	**53.5%**	*	4.6	**42.2%***	
ABCB6	A549	183.2	151.1	82.5%	49.8	**27.2%**	*	48.2	**31.9%***	
	BEAS-2B	7.0	7.0	99.6%	5.5	79.3%		2.2	**31.8%***	

* and **bold** indicates significant change in gene expression vs. CTL ($p<0.05$, t-test, n=3-6)

NRF2 silencing led to significantly reduced expression of 6 of 7 known, and 5 of 6 putative NRF2-regulated genes in both A549 and BEAS-2B cells ($p<0.05$, t-test; see Supplementary Table S5). For many genes, we observed mRNA reduction with NRF2 silencing at both baseline and after SFN treatment consistent with high baseline NRF2 activity in these cell lines. SFN-induced gene expression of known and putative genes in A549 cells was modest. Of the 13 tested known and putative NRF2-regulated genes, only *HMOX1, MAFG, SLC7A11,* and *OSGIN1* gene expression displayed significant increase in A549 cells, whereas 9 of the 13 known or putative NRF2-genes were induced in BEAS-2B cells by an average of 764%.

Supplementary Table S5 (cont). Expression values for 30 candidate genes in NRF2-silenced cell lines.

		mRNA Expression Values (normalized to β-actin x100)								
		Control siRNA				NRF2 siRNA				
Gene Name	Cell line	Baseline	SFN	% change up/down		Baseline	% control siRNA		SFN	% control siRNA	
Gene expression significantly reduced by siRNA in both cell lines											
ABHD4	A549	16.6	35.1	211.9%	*	10.2	61.5%	*	12.0	34.3%	*
	BEAS-2B	11.7	17.3	148.2%	*	6.3	54.2%	*	7.4	42.9%	*
AIFM2	A549	11.8	9.8	83.4%	*	5.0	42.5%	*	3.3	33.8%	*
	BEAS-2B	5.9	7.2	122.1%	*	3.0	50.7%	*	3.0	41.8%	*
AMBP	A549	3.4	2.3	68.1%	*	0.8	23.7%	*	0.5	21.4%	*
	BEAS-2B	0.1	0.1	81.1%	*	0.1	67.3%	*	0.1	66.1%	*
BACH1	A549	0.5	0.6	100.7%	*	0.3	51.5%	*	0.2	29.3%	*
	BEAS-2B	0.4	0.4	118.9%	*	0.3	72.7%	*	0.3	60.1%	*
CREBZF	A549	9.0	10.0	110.6%	*	5.5	61.4%	*	6.0	59.8%	*
	BEAS-2B	4.1	3.1	74.7%	*	4.3	105.1%	*	1.8	59.5%	*
FBXO30	A549	4.1	5.8	140.4%	*	2.0	49.6%	*	1.9	33.6%	*
	BEAS-2B	1.3	2.7	207.7%	*	1.2	93.5%	*	1.7	64.3%	*
FECH	A549	5.5	4.5	82.9%	*	3.8	70.2%	*	2.6	57.8%	*
	BEAS-2B	6.8	6.2	91.5%	*	5.5	80.6%	*	4.4	70.7%	*
GABARAPL1	A549	11.3	19.0	167.2%	*	8.1	71.7%	*	6.4	33.8%	*
	BEAS-2B	4.8	8.2	172.6%	*	2.7	56.7%	*	3.1	37.5%	*
GAPDH	A549	182.1	150.1	82.4%	*	102.3	56.2%	*	90.2	60.1%	*
	BEAS-2B	27.4	29.0	105.9%	*	27.7	101.2%	*	15.6	53.9%	*
GHITM	A549	75.0	72.7	96.9%	*	36.5	48.6%	*	33.6	46.2%	*
	BEAS-2B	30.1	29.7	98.7%	*	18.5	61.5%	*	16.0	54.0%	*
GNPDA1	A549	20.1	22.7	113.0%	*	12.0	59.9%	*	14.2	62.8%	*
	BEAS-2B	4.3	5.2	123.2%	*	2.4	56.2%	*	2.7	52.1%	*
HTATIP2	A549	27.4	20.4	74.5%	*	8.4	30.5%	*	6.5	32.0%	*
	BEAS-2B	2.9	5.6	193.8%	*	1.5	52.5%	*	2.5	45.8%	*
LBR	A549	0.3	0.8	304.9%	*	nd	10.2%	*	nd	4.5%	*
	BEAS-2B	0.2	1.0	460.4%	*	nd	<1%	*	nd	<1%	
NCAPD2	A549	32.4	35.6	110.0%	*	3.4	10.5%	*	5.0	14.0%	*
	BEAS-2B	26.0	18.1	69.7%	*	18.7	71.8%	*	13.9	76.9%	*
RFFL	A549	3.1	3.8	124.1%	*	1.5	47.4%	*	1.2	31.9%	*
	BEAS-2B	0.8	0.8	101.6%	*	0.4	50.6%	*	0.4	48.6%	*
RXRA	A549	89.5	77.4	86.5%	*	43.3	48.4%	*	57.7	74.5%	*
	BEAS-2B	6.0	4.3	71.0%	*	6.3	104.2%	*	2.5	58.6%	*
SLC3A2	A549	196.2	187.8	95.7%	*	97.7	49.8%	*	124.7	66.4%	*
	BEAS-2B	89.8	109.8	122.3%	*	84.8	94.4%	*	75.9	69.1%	*
TFE3	A549	11.0	14.1	128.1%	*	6.7	61.2%	*	9.7	68.6%	*
	BEAS-2B	10.1	10.3	101.8%	*	6.0	59.5%	*	6.8	66.1%	*
TNFSF9	A549	11.7	10.9	93.5%	*	6.9	58.5%	*	6.3	57.9%	*
	BEAS-2B	1.5	3.0	199.1%	*	1.2	81.7%	*	1.3	42.3%	*
UNKL	A549	0.3	0.2	55.8%	*	0.1	39.2%	*	nd	<1%	*
	BEAS-2B	0.1	0.1	183.0%	*	nd	60.4%	*	nd	33.5%	*

***** indicates significant change in gene expression vs. CTL ($p<0.05$, t-test, n=3-6)
- No detectable expression

NRF2 silencing significantly altered expression of 20 of 30 of the candidate genes in both A549 and BEAS-2B cells including *RXRA*

S5
Continued

		mRNA Expression Values (normalized to β-actin x100)						
		Control siRNA			NRF2 siRNA			
Gene Name	Cell line	Baseline	SFN	% change up/down	Baseline	% control siRNA	SFN	% control siRNA
Gene expression significantly reduced by siRNA in one cell line								
GPD2	A549	8.9	9.3	104.1%	5.5	61.8%	5.3	56.8%*
	BEAS-2B	2.0	1.6	80.0%	1.5	75.1%	1.1	70.4%
NDUFAF4	A549	7.8	9.3	118.3%	7.3	93.6%	7.5	81.4%
	BEAS-2B	5.1	5.5	107.0%	3.4	65.8%*	2.8	50.4%*
HIST1H4H	A549	2.7	2.4	87.9%	2.9	105.1%	2.7	112.7%
	BEAS-2B	3.1	2.2	70.1%	1.9	61.0%	1.4	64.7%*
Gene expression induced								
MT2A	A549	111.0	70.0	63.0%	239.1	215.5%*	210.4	300.8%*
	BEAS-2B	60.6	46.1	76.0%	42.6	70.2%	33.3	72.4%
BEND6	A549	2.8	3.3	118.4%	1.7	60.1%	4.2	127.1%
	BEAS-2B	0.4	0.7	151.0%*	0.6	131.4%*	0.5	82.2%
No Change								
BRD2	A549	10.4	13.4	129.6%	10.0	96.4%	10.0	74.3%
	BEAS-2B	1.1	0.7	61.5%	0.8	75.9%	0.6	94.9%
DGAT2L6	A549	-	-	-	-	-	-	-
	BEAS-2B	-	-	-	-	-	-	-
P4HTM	A549	-	-	-	-	-	-	-
	BEAS-2B	-	-	-	-	-	-	-
TINAG	A549	-	-	-	-	-	0.1	-
	BEAS-2B	-	-	-	-	-	-	-
WRD81	A549	1.4	1.3	89.9%	01.3	96.5%	0.8	63.6%
	BEAS-2B	0.8	0.7	93.0%	0.7	83.5%	0.8	104.2%

***** indicates significant change in gene expression vs. CTL ($p<0.05$, t-test, n=3-6)
- No detectable expression

Supplementary Table S6. Primers designed for real-time qPCR expression assays and ChIP-PCR.

Gene target	FWD primer sequence (5' -> 3')	REV primer sequence (5' -> 3')
ABCB6	CAGCTATGCCGATGGGCGGG	AATGGCGACGCGCTGCTTCT
ABHD4	AGCCCCGAGCAAAACGACCG	CACCAGACCAGGCCCCCAGG
AIFM2	CAGGCCTACAAGCCGGGTGC	TTCTCCCGCCTGGCCTCTCC
AMBP	CTGCCAAGCTCTACGGGCGG	TACCGTTGCCCATGCAGCCG
BACH1	AAGCCTCGCACAATATGGTTGATGA	CGGAACCGCTGTCCCTCCAC
BEND6	TGGCCGGGTGCCTCTAGCTT	TGCTTTCCCCGGCTGCATTCT
BRD2	GGTGATGTGGCGTGTGGGGG	TCCAGCACTCTCTCCCCGCC
CREBZF	CGGTGGAGTTCTGCTCGGCG	CCAGGGTGGACAGGGCCCAA
DGAT2L6	CCCACAGTCAAGGTGGCAGGC	AGTGGAGGCTCCTGGTCGGC
FBXO30	CCGGCCGAGCTGGACTGGC	TCCCTGGCTCTGGCCTGGTC
FECH	ACCGCAGAAGAGGAAGCCGA	TTGGGGGTTCGGCGTTTGGC
FTH1	GAGACCACAAGCGACCCGCA	CGGCCACCTCGTTGGTTCTGC
FTL	CCGCACGGACCCCCATCTCT	TACTCGCCCAGCCCAGCCTC
GABARAPL1	CCGGACAGGGTCCCCGTGAT	TCCCCATGTCGCGCACACAC
GHITM	GTGACCGGGGACCGAGCATT	TCTCCCACGCCGGATCCCAA
GNPDA1	CGGGAGGCGTCCGTGACAAG	GTGGGGAGCCCCAGGGTGAA
GPD2	GCGCGTGAGGATCTATCTCAGGCTAA	TGGCACGCTCATGAAGGGCT
HIST1H4H	GCACGCCAAACGCAAGACCG	AGAGTGCAGCAAGCAGGAGCC
HTATIP2	TTTTGGGCGCCAGCGGAGAA	ACAAATCCCTCCGCCCCAGC
KEAP1	CCATGGCGGGGTCCCTGAGT	TGCGGTTGCCATGCTGGGAG
LBR	AGCCCCTCCTCGCAGCGTTA	CCTCGGCGTCTGGAAGGGGA
MAFG	CCCTTGTCTTGCGCCTGCCT	CCGGCTCCCGCTTCACCTTC
MT2A	CTGCGCCGCCGGTGACT	GCAAACGGTCACGGTCAGGGT
NCAPD2	TCTGCCAGAGCCAAGGCCCA	GCAGGCGACCTTCTCGGTGG
NDUFAF4	GTTCCCACGTGCGGCCTGAA	GCAGCTTTTACCTGCAAGGAAGACA
OSGIN1	CTGCCTGTCAGGTCCGCTGC	GCGTGCTCCTTCCGGTGCTT
P4HTM	TCCCAACTGGGGGCTGCCTT	CACCCACCCAACCTTGCCCA
PIR	TGCAGGGGTCCACTAGCCCT	TCAGCGTGCAGAATGCCCCG
PRDX1	CCCCACGTAGGTGCGGGAAC	AAGGCCCCTGAACGAGATGCC
PSMA3	TGGCTGCAGTTTCATGTTAGGGTC	GCCGATGGCACAGCCCCAAT
RFFL	CCAGCGACCTCAGCCACAGG	GCAGGTCTGCTTCCTGGCCG
RXRA	TGAAGCGGGAAGCCGTGCAG	GGTGACAGGGTCGTTCGGCG
SLC3A2	GCCGGTTCTGCAGGCACCAT	CCTTCAGACCCGCCAGGTTGC
SLC7A11	GGCTGCCTTCCCTGGGCAAC	CAGCAGTAGCTGCAGGGCGTA
TALDO1	GGAGCTGGTGGAGGAGGCGA	CCTCTTGTGACCCGCCCAGC
TFE3	GACTGCAGCTCCCCAGCACG	TCCAGCGCATCTCCGGGTCA
TINAG	CGCCTTGGCACTTTGCCACC	CGGTCAGCAGCCACACTTGC
TNFSF9	CTGCGGCAGGGCATGTTTGC	CCAAGACTGTGGCGCCCTGG
UNKL	GGGAGCAGCAGGTCCCAGGT	CGGCTCTGAACGCAGGGGTG
WDR81	CAGCGCGCTCTGTGCTGGC	TCTGGAGCCCGCTCCTCACC

Supplementary Table S6. (Continued)

ChIP PCR Primers

Gene target	FWD primer sequence (5' -> 3')	REV primer sequence (5' -> 3')	Fold enrichment Target/Neg Control NQO1	High Confidence/ ChIP Peak Rank
ABHD4	TAGGTGGTGTGACTAGCAGTTCGC	CTGGGTCCAGGAAAGGCCCAGT	1.82	Rank 427
AIFM2	CGCTCCCGCTTGGTCGTCTT	GAGTGCTGAGTCACGCCCCG	2.73	HC/ Rank 64
AMBP	CCCACAGAGGGCATGCGAGG	ATGGGCCCAATCAGGCTTGACC	2.15	Rank 332
FBXO30	ACGTCACGGCATTAAAGTGCTAGG	GCGGTTTCCGCTGAATCACTCT	1.96	Rank 829
FECH	AGGCCAGGCAGAGACACG	TAGTTTGGCAGATGCAAACAGGGC	1.95	HC/ Rank 136
HMOX1	CCCTGCTGAGTAATCCTTTCCCGA	ATGTCCCGACTCCAGACTCCA		HC/Rank 7, (Positive Control)
HTATIP2	TATGCCCAGTGATGCCAGCAGCTT	AGGAGGATATTGTTCTCCGCAGTC	2.31	HC/ Rank 54
KEAP1	GCGCGCAGGTCACCATGACT	GTCCCTACCGCCTGAGGCCA	10.62	HC/Rank 8
NQO1	CCCTTTTAGCCTTGGCACGAAA	TGCACCCAGGGAAGTGTGTTGTAT	5.42	HC/ Rank 3 (Positive Control)
NQO1 Upstream	TAAAAAGTAGAGTGGTTGGAGTGATGACG	TCTCAGTTTTTGCCCTTATTTAATCCC	1	Neg Control
OSGIN1	TTTAAGGCTGGCCATGAGGC	AGAGGGAAGTGAGGGTATTTCACG	2.51	Rank 287
P21 Upstream	GAGTCTTGCTCAGTGGGAGCTCTGGGAGTA	ATGTGACTTGGGGTGAGGCCTACTCGG	-	Neg Control
PIR	TTTGCAAACTGACCGCCAGCATTC	ACTGGACCCACACTCTCTTAACCT	7.15	HC/Rank 17
PMAIP1	GGGTGACGGACATGGCCCCT	CGCTCCACTGCCTTCAGCCC	1.8	HC/Rank 32
PPARGC1B	CTCCAGCTCCCACGCTGTGC	CCAGCCTGGGCTTGTCAGCC	4.15	HC/Rank 36
PRDX1	GCTGCCTTTATAGCCAGTAGGGAT	AACCTCAGCCATCCGCAACA	3.29	HC/Rank 31
RXRA	GGGTTTGCAGAAGTGGAGGCT	AACAGCTGCAGCGTGCAGTGACA	3.83	HC/ Rank 6
TNFSF9	AAGCGGAGAGAGATCCGAGTGG	AGAGCCTTTCCCCTCGTCCCC	2.02	Rank 849
UNKL	TCAGCCCCGGGCGTTAGGAAA	AGCTTGTCCTCGCGTGTCCCT	2.84	HC/ Rank 37
	Mouse primers tested in 3T3-L1 cells			
Mm NQO1	AGTCACCTTTGCACGCTAGG	TCTAAGAGCAGAACGCAGCA	-	Positive Control
Mm p21UP	GATACTCCCAGGGAAAGGATCCCTT	GTGCACACTGCGAATTCACGGG	-	Neg Control
Mm RXRa	GATAGGCAGGCTGAGGGAAG	GTGGGAAACTCACCCTGTCA	-	HC

Materials and Methods

Cell culture

We grew human lymphoblastoid cells (Coriell) as recommended by Coriell. Beas2B, A549 and 3T3-L1 cells were grown as recommended by ATCC. LCLs were grown in RPMI 1640 supplemented with 15% heat-inactivated fetal bovine serum (Invitrogen) and 1X antibiotics/antimycotics (Gibco) at 5% CO2 at 37°C. BEAS-2B cells (ATCC CRL-9609) were grown in RPMI 1640 supplemented with 10% fetal bovine serum (Invitrogen), 2.5mM L-glutamine (Invitrogen) and 1X antibiotics/antimycotics at 5% CO2 at 37°C. We grew A549 cells (ATCC CCL-185) in Ham's F12K supplemented with 10% fetal bovine serum and 1X antibiotics/antimycotics at 5% CO2 at 37°C.

For ChIP experiments, we treated lymphoblastoid cells at a density of 900,000 cells/ml with 10 μM D,L-sulforaphane (Calbiochem) or 0.1% (v/v) DMSO as a vehicle control for 5 h. We covalently cross-linked proteins to DNA by incubating cells in 1% formaldehyde (10 min) followed by 0.125 M glycine (5 min, room temp) to halt cross-linking reaction. Cells were pelleted at 1350 g (5 min, 4°C), aspirated, and washed twice with ice-cold PBS (pH 7.4). The final pellet wash was in PBS with protease inhibitors (Roche) followed by snap-freezing in liquid nitrogen and storage at -80°C.

To prepare RNA for microarray and real-time PCR experiments, we treated cells with SFN as above. We collected the cells by pelleting at 1350 g, washed twice with PBS (pH 7.4) and then lysed the pellets in buffer RLT (Qiagen) + 1% β-mercaptoethanol. Lysates were homogenized with QIAshredder columns (Qiagen) and RNA was isolated using Qiagen's RNeasy kit including an on-column DNA digestion step per manufacturer's instructions. RNA was quantified using RiboGreen (Invitrogen) and stored at -80°C.

3T3-L1 Differentiation

3T3-L1 preadipocytes were obtained from ATCC (Manassas, VA) and grown in high-glucose Dulbecco's modified Eagle's medium (DMEM) with 1X antibiotics/antimycotics, and 10% FBS. 3T3-L1 cells were grown until confluent (designated as day 0) and differentiation process was initiated by replacing growth medium with differentiation medium containing DMI cocktail (32,36,37). DMI differentiation medium contains 1 μM dexamethasone, 0.5 mM IBMX and 5 μg/ml insulin in DMEM with 10% FBS. After 48 h the medium was replaced with DMEM with 10% FBS supplemented with 1 μg/ml insulin. The cells were kept for an additional 5 days by replacing medium every two days with DMEM with 10% FBS supplemented with 1 μg/ml insulin. Oil red O lipid staining (ORO) was used to assess the differentiated adipocytes following the protocol described in Pi et al (32). Mature adipocytes were visualized by phase contrast microscopy at a magnification of 200X. Cells were maintained at 37 °C in a 5% CO2 environment. 3T3-L1 cells with stable shRNA knockdown for Nrf2, Keap1 and scramble shRNA were generated as described in Pi et al (32). Insulin solution (human, I9278), 3-isobutyl-1-methylxanthine (IBMX, I7018), dexamethasone (D1756), were obtained from Sigma (St. Louis, MO). D,L-sulforaphane from Calbiochem.

Chromatin immunoprecipitation (ChIP)

For each tested lymphoblastoid cell line (6 total), we performed ChIP in biological duplicate or triplicate and combined replicates after validating SFN-induced NRF2 binding at known ARE loci for every experiment (see Figure 1B). To perform ChIP, methods and buffers were taken from Agilent's Mammalian ChIP-on-Chip protocol (Agilent, Version 10.0, May 2008). Briefly, we lysed pellets containing 5 X 107 cross-linked lymphoblastoid cells, fragmented the chromatin to an average size of 200-500 bp with a Misonix 3000 sonicator (30 pulses, 30 s on, 20 s off, 100% power), and centrifuged to recover the supernatant. We immunoprecipitated DNA-bound protein using a rabbit monoclonal antibody specific for the C-terminus of human NRF2 (Epitomics, Clone ID EP1808Y) or a non-specific rabbit IgG antibody (Invitrogen) conjugated to goat anti-rabbit IgG magnetic beads (Invitrogen). For each 5 X 107 isolated nuclei, we immunoprecipitated with primary Ab/secondary Ab bead complexes overnight (4°C), washed the protein-bound beads, and then reversed the formaldehyde cross-links and eluted the chromatin (overnight, 65°C). RNA and protein were digested, and the DNA extracted using phenol chloroform and phase lock gel (Sigma-Aldrich). DNA was further purified using Qiaquick PCR Purification Kit (Qiagen) according to the manufacturer's instructions, dried down using a SpeedVac and resuspended in double-distilled H2O. We quantified ChIP DNA using PicoGreen (Invitrogen).

ChIP-seq

The yield of ChIP DNA for individual ChIP experiments was in the range of 200-600pg. After a preliminary sequencing experiment we determined we needed to increase the amount of ChIP DNA used for library construction and sequencing and we pooled DNA from replicates and some cell lines. Therefore in each sequencing run of NRF2-antibody precipitated DNA, we combined ChIP DNA from replicates of two separate lymphoblastoid cell lines that had been immunoprecipitatied in parallel experiments (GM06993 and GM12872; GM07000 and GM11882; GM11992 and GM12763). We prepared input DNA and IgG-precipitated samples (vehicle-control and SFN treated) from a pool of ChIP DNA from all 6 cell lines combined. Because single nucleotide polymorphisms (SNPs) are known to affect transcription factor binding (19), this pooling strategy has the additional benefit of minimizing any impact from SNPs. Following the pooling we had 1-5 ng of ChIP DNA for each library and these were prepared using the standard Illumina ChIP-seq protocol. ChIP-seq in Beas2B cells used the same approach. We sequenced 11 lanes in total, including 4 NRF2 antibody precipitated vehicle-control treated samples, 4 NRF2 antibody precipitated SFN treated samples, 2 IgG antibody precipitated control samples, and input DNA (Supplementary Table S1, input sequences from ENCODE were also compared in Table S2). The National Center for Genome Resources (Santa Fe, NM) created the libraries and sequenced the immunoprecipitated samples on the Illumina Genome Analyzer II. Briefly, sequencing adapters were ligated to immunopreciptated DNA, and then size-selected by gel electorophoresis (250 +/- 25 bp). Fragments were then amplified by 18 cycles of PCR. The samples were then sequenced, and short reads were mapped to NCBI human reference genome (build 36.3, March 2008) using Burrows-Wheeler Alignment (BWA) Tool (38). By default, BWA finds an alignment (ungapped and gapped) with maximum edit-distance of 2 to the 36 bp query sequence, disallowing gaps close to the end of the query. Sequencing data has been deposited to the NCBI GEO database (http://www.ncbi.nlm.nih.gov/geo/) .

ChIP-seq Data Analysis

The uniquely mapped short reads were used to identify regions of the genome with significant enrichment in NRF2-associated DNA sequences, hereafter referred to as 'peak regions' owing to their appearance in

genome-wide density plots. The peak detection was performed by QuEST 2.4 software (39) using the "Transcription factor binding site" setting (bandwidth of 30 bp, region size of 300 bp) and the "stringent peak calling" parameters (corresponding to 50-fold ChIP to input enrichment for seeding the regions, and 3-fold ChIP enrichment for extending the regions). The three sequenced lanes were examined individually for reproducibility and then unique reads were combined and reanalyzed to produce composite binding regions.

Gene expression microarray

To measure whole-genome expression, we used Illumina HumanRef-8 v.3.0.Expression BeadChips which measures 24,500 transcripts (based on NCBI RefSeq build 36.2). We exposed 60 lymphoblastoid cell lines to vehicle control or 10 μM SFN for 24 h in biological triplicate and isolated RNA from these samples using Qiagen RNeasy kit with the DNase digestion step. After quantification with RiboGreen (Invitrogen), we biotin-labeled 850 ng of RNA from each sample using Illumina TotalPrep RNA Amplification Kit (Ambion) according to manufacturer's instructions. We hybridized, washed and detected signal according to Illumina's Whole-Genome Gene Expression protocol (revision D). We extrapolated data from images taken by the reader using BeadStudio (Illumina). Summary data from Illumina's Beadstudio were read using the beadarray R package (87) and then normalized on a log scale using a quantile normalization method across replicates of a single individual, followed by a median normalization method across individuals (88). The averaged log2 intensities of the biological replicates were used in subsequent analyses. We eliminated probes from further analysis that were not "significantly expressed" (i.e., we kept probes in which at least 75% samples had detection p-value less than 0.05). We considered the gene transcriptional response significant if expression after treatment had a fold change greater than or equal to 1.3 or less than or equal to 0.7 compared to vehicle-control levels and q-value < 0.05 after False Discovery Rate adjustment (89).

De novo motif discovery and identification of putative NRF2 binding sites

In order to determine if our ChIP-seq experiment allows unambiguous recovery of the DNA motif responsible for sequence-specific NRF2 protein-binding, we applied de novo motif discovery to the ChIP-seq peak regions. Using the Gibbs motif sampler (41, 42), we searched all regions for enriched sequence patterns without any assumption. To identify putative NRF2 binding sites, we used a position weight matrix method based on a curated list of known AREs, as previously described (19).

Western blot

We grew cell lines in 100 mm petri dishes and isolated nuclear and cytoplasmic extracts using the Active Motif Nuclear Extraction kit according to manufacturer's instructions and quantified the protein extracts by Bradford assay (Bio-Rad). We electrophoresed 30 μg nuclear extract and 50 μg cytoplasmic with a 4-12% gradient Tris-Bis gel (Invitrogen) and then transferred the protein to a 0.2 μM nitrocellulose membrane (Invitrogen). We blocked the membrane in 5% milk and 1X TBST (Sigma; 2 h, 4°C), and then probed the membranes with 1:1000 anti-NRF2 rabbit polyclonal (Santa Cruz Biotechnologies, sc-13032), 1:2000 anti-βactin mouse monoclonal (Sigma-Aldrich, A5316), anti-TATA binding protein (Abcam, 1TBP18), anti-HSP90 (BD Transduction Laboratories) in 5% milk in TBST (overnight, 4°C). After washing, we probed the bound antibodies with 1:5000 anti-rabbit or anti- mouse HRP-conjugated secondary antibodies (BioRad, 170-5046 and 170-5047, respectively) in TBST (2 h, room temp) in 5%

milk. After final washing of the membrane, we incubated for one minute in ECL solution (Pierce) and exposed to film.

Real-time quantitative polymerase chain reaction (qPCR)

We isolated ChIP DNA, as described above, and tested for enrichment of known ARE loci HMOX1 and NQO1. Primers previously were designed to span three known AREs in HMOX1 promoter (90). In addition, we designed primers to amplify the human NQO1 ARE (91) (Fwd 5'-CCCTTTTAGCCTTGGCACGAAA-3', Rev 5'- TGCACCCAGGGAAGTGTGTTGTAT-3') and a negative control region approximately 3000 bp upstream of the NQO1 ARE (Fwd 5'-TAAAAAGTAGAGTGGTTGGAGTGATGACG-3', Rev 5'-TCTCAGTTTTTGCCCTTATTT AATCCC-3'). We added 3 µl of ChIP DNA and 200 nM of each primer to Power SYBR PCR Master Mix (ABI) in technical triplicate. As a control, we also tested 1:100 diluted input DNA. To normalize, we divided target values from ChIP samples with matched input samples. We determined enrichment of ARE loci by comparing the normalized values of HMOX1 and NQO1 ARE loci to the NQO1 upstream locus.

For gene-specific expression analysis, we isolated total RNA isolated using the RNeasy kit (Qiagen) and treated with DNase. We reverse transcribed cDNA using SuperScript First-Strand Synthesis System (Invitrogen) with poly-T primers following manufacturers' instructions. We used TaqMan gene expression assays (Applied Biosystems) for NRF2 (Hs00232352), NQO1 (Hs00168547), HMOX1 (Hs00157965), GAPDH (Hs99999905), and BACT (Hs99999903). For others, we designed primers to span exon junctions for each target gene using Primer3 (92) (see Supplementary Table S8), and normalized target values with ACTB mRNA measurements.

For both qPCR and reverse transcriptase qPCR amplifications, we ran 40 PCR cycles using 15 seconds 95°C melting temperature and 1 minute optimal (60°C-69°C) annealing/extension temperature per cycle. We measured fluorescence intensity with an ABI 7900HT and calculated initial fluorescence (Ro value) of each amplified sample using the method described by Peirson and colleagues (93). All measurements were performed in at least triplicate and reported as the average values ± standard error of the mean.

NRF2 gene silencing

We silenced NRF2 in BEAS-2B and A549 cells using a reverse transfection protocol. For BEAS-2B cells, we trypsinized cells from an actively growing culture and transfected 1 X 105 cells with 0.4 µg NRF2 siRNA (Ambion, ID # 115764) or non-targeting control siRNA (Ambion, AM4643) in the presence of 1 µl FuGENE Xtreme Gene siRNA transfection reagent (Roche) for each well of a 12-well plate. For A549 cells, we transfected 3-5 X 104 cells with 0.3 µg siRNA in the presence of 2 µl Lipofectamine 2000 transfection reagent (Invitrogen) for each well of a 12-well plate. We seeded transfected cells in antibiotic-free RPMI (BEAS-2B) or Ham's F12K (A549) media with 10% FBS and incubated from 24-48 hours before 8 hour 10 µM SFN or 0.1% DMSO vehicle-control treatment. Nrf2 and Keap1 were silenced in 3T3-L1 cells using shRNA as described in Pi et al (32).

Supplementary References

87. Dunning, M.J., Smith, M.L., Ritchie, M.E. and Tavare, S. (2007) beadarray: R classes and methods for Illumina bead-based data. Bioinformatics, 23, 2183-2184.
88. Bolstad, B.M., Irizarry, R.A., Astrand, M. and Speed, T.P. (2003) A comparison of normalization methods for high density oligonucleotide array data based on variance and bias. Bioinformatics, 19, 185-193.
89. Benjamini, Y. and Hochberg, Y. (1995) Controlling the False Discovery Rate: A Practical and Powerful Approach to Multiple Testing. Journal of the Royal Statistical Society. Series B (Methodological), 57, 289-300.
90. Keum, Y.S., Yu, S., Chang, P.P., Yuan, X., Kim, J.H., Xu, C., Han, J., Agarwal, A. and Kong, A.N. (2006) Mechanism of action of sulforaphane: inhibition of p38 mitogen-activated protein kinase isoforms contributing to the induction of antioxidant response element-mediated heme oxygenase-1 in human hepatoma HepG2 cells. Cancer Res, 66, 8804-8813.
91. Dhakshinamoorthy, S., Long, D.J., 2nd and Jaiswal, A.K. (2000) Antioxidant regulation of genes encoding enzymes that detoxify xenobiotics and carcinogens. Curr Top Cell Regul, 36, 201-216.
92. Rozen, S. and Skaletsky, H. (2000) Primer3 on the WWW for general users and for biologist programmers. Methods Mol Biol, 132, 365-386.
93. Peirson, S.N., Butler, J.N. and Foster, R.G. (2003) Experimental validation of novel and conventional approaches to quantitative real-time PCR data analysis. Nucleic Acids Res, 31, e73. doi:10.1093/nar/gng1073.
94. Erickson, A.M., Nevarea, Z., Gipp, J.J. and Mulcahy, R.T. (2002) Identification of a variant antioxidant response element in the promoter of the human glutamate-cysteine ligase modifier subunit gene. Revision of the ARE consensus sequence. J Biol Chem, 277, 30730-30737.
95. Arinze, I.J. and Kawai, Y. (2005) Transcriptional activation of the human Galphai2 gene promoter through nuclear factor-kappaB and antioxidant response elements. J Biol Chem, 280, 9786-9795.
96. Banning, A., Deubel, S., Kluth, D., Zhou, Z. and Brigelius-Flohe, R. (2005) The GI-GPx gene is a target for Nrf2. Mol Cell Biol, 25, 4914-4923.
97. Dhakshinamoorthy, S., Jain, A.K., Bloom, D.A. and Jaiswal, A.K. (2005) Bach1 competes with Nrf2 leading to negative regulation of the antioxidant response element (ARE)-mediated NAD(P)H:quinone oxidoreductase 1 gene expression and induction in response to antioxidants. J Biol Chem, 280, 16891-16900.
98. Hintze, K.J. and Theil, E.C. (2005) DNA and mRNA elements with complementary responses to hemin, antioxidant inducers, and iron control ferritin-L expression. Proc Natl Acad Sci U S A, 102, 15048-15052.
99. Kim, Y.C., Yamaguchi, Y., Kondo, N., Masutani, H. and Yodoi, J. (2003) Thioredoxin-dependent redox regulation of the antioxidant responsive element (ARE) in electrophile response. Oncogene, 22, 1860-1865.
100. Kurz, E.U., Cole, S.P. and Deeley, R.G. (2001) Identification of DNA-protein interactions in the 5' flanking and 5' untranslated regions of the human multidrug resistance protein (MRP1) gene: evaluation of a putative antioxidant response element/AP-1 binding site. Biochem Biophys Res Commun, 285, 981-990.

101. Lesniak, W., Szczepanska, A. and Kuznicki, J. (2005) Calcyclin (S100A6) expression is stimulated by agents evoking oxidative stress via the antioxidant response element. Biochim Biophys Acta, 1744, 29-37.
102. Li, Y. and Jaiswal, A.K. (1992) Regulation of human NAD(P)H:quinone oxidoreductase gene. Role of AP1 binding site contained within human antioxidant response element. J Biol Chem, 267, 15097-15104.
103. Moinova, H.R. and Mulcahy, R.T. (1998) An electrophile responsive element (EpRE) regulates beta-naphthoflavone induction of the human gamma-glutamylcysteine synthetase regulatory subunit gene. Constitutive expression is mediated by an adjacent AP-1 site. J Biol Chem, 273, 14683-14689.
104. Montano, M.M., Deng, H., Liu, M., Sun, X. and Singal, R. (2004) Transcriptional regulation by the estrogen receptor of antioxidative stress enzymes and its functional implications. Oncogene, 23, 2442-2453.
105. Mulcahy, R.T., Wartman, M.A., Bailey, H.H. and Gipp, J.J. (1997) Constitutive and beta-naphthoflavone-induced expression of the human gamma-glutamylcysteine synthetase heavy subunit gene is regulated by a distal antioxidant response element/TRE sequence. J Biol Chem, 272, 7445-7454.
106. Munzel, P.A., Schmohl, S., Buckler, F., Jaehrling, J., Raschko, F.T., Kohle, C. and Bock, K.W. (2003) Contribution of the Ah receptor to the phenolic antioxidant-mediated expression of human and rat UDP-glucuronosyltransferase UGT1A6 in Caco-2 and rat hepatoma 5L cells. Biochem Pharmacol, 66, 841-847.
107. Park, E.Y. and Rho, H.M. (2002) The transcriptional activation of the human copper/zinc superoxide dismutase gene by 2,3,7,8-tetrachlorodibenzo-p-dioxin through two different regulator sites, the antioxidant responsive element and xenobiotic responsive element. Mol Cell Biochem, 240, 47-55.
108. Tsuji, Y. (2005) JunD activates transcription of the human ferritin H gene through an antioxidant response element during oxidative stress. Oncogene, 24, 7567-7578.
109. Wang, Y., Xiao, L., Thiagalingam, A., Nelkin, B.D. and Casero, R.A., Jr. (1998) The identification of a cis-element and a trans-acting factor involved in the response to polyamines and polyamine analogues in the regulation of the human spermidine/spermine N1-acetyltransferase gene transcription. J Biol Chem, 273, 34623-34630.
110. Wilson, L.A., Gemin, A., Espiritu, R. and Singh, G. (2005) ets-1 is transcriptionally up-regulated by H2O2 via an antioxidant response element. Faseb J, 19, 2085-2087.
111. Yueh, M.F. and Tukey, R.H. (2007) Nrf2-keap1 signaling pathway regulates human UGT1A1 expression in vitro and in transgenic UGT1 mice. Faseb J, 21, A1182-A1182.
112. Weerachayaphorn, J., Cai, S.Y., Soroka, C.J. and Boyer, J.L. (2009) Nuclear factor erythroid 2-related factor 2 is a positive regulator of human bile salt export pump expression. Hepatology, 50, 1588-1596.